# A Sequential Testing Framework for Identifying a Transmission Line Outage in a Power System

### Kuraganti Chetan Kumar
chatan@iisc.ac.in
Indian Institute of Science
Bangalore, Karnataka, India

### Gurunath Gurrala
gurunath@iisc.ac.in
Indian Institute of Science
Bangalore, Karnataka, India

### Rajesh Sundaresan
rajeshs@iisc.ac.in
Indian Institute of Science
Bangalore, Karnataka, India

## ABSTRACT

The topology of a power system changes when a line outage is encountered. Identifying which line has failed in the shortest possible time is of importance due to the cascading nature of such failures. In this work, we propose a state estimation based sequential hypothesis testing procedure to locate the failed line. We focus on single line outages as these are the most frequently occurring failures. Earlier work on state estimation based sequential testing procedure used a DC approximation model assuming that the sensors provided angle and voltage information. This is known to be a coarse model but results in a simpler linear estimation problem. In this work, we look at a finer nonlinear model of power measurements and treat phase angles and voltages as hidden states. After a local linearization, we propose a Kalman filter based state estimation followed by a generalized likelihood ratio testing procedure to determine which of the lines has failed. We consider both centralized and decentralized approaches. In the centralized case, measurements from every installed meter is made available to the system operator. In the decentralized case, only limited aggregated information is made available because of, for example, communication capacity constraints. We test our algorithms on the IEEE 14 and 118 bus systems and show that all high risk link failures are quickly identified.

## CCS CONCEPTS

• **General and reference** → **Estimation**; *Measurement*; • **Mathematics of computing** → **Hypothesis testing and confidence interval computation**; **Kalman filters and hidden Markov models**; *Time series analysis*.

## KEYWORDS

Topology identification, Kalman filtering, Decentralized state estimation, Sequential hypothesis testing, Unscented Kalman filter.

## 1 INTRODUCTION

A power system is a network of a large number of substations, transformers and transmission lines. A transmission line outage due to faults could overload other transmission lines leading to cascading failures [11, 16]. Examples include the US-Canada blackouts in 2003 [14], the Arizona - Southern California outages in 2011 [13], the Italy and Switzerland blackouts in 2003 [30] and the North Indian blackout [5, 24]. If grid operators have sufficient tools to identify single line outages in real time, immediate corrective action can be taken, and the cascading failures leading to blackouts could can be prevented. Towards this, operating conditions of a power system are monitored by Supervisory Control And Data Acquisition (SCADA) systems. These provide critical telemetry data on transmission line statuses and network topology. Despite such safeguards, there have been at least two blackout instances (North America, 2003 and 2011) caused by erroneous records and telemetry data. Certain lines in the network were either overloaded or were near overload in the 2011 blackout, yet operators could not detect these because the model was not up-to-date which resulted in inaccurate state estimates [13]. Reliable signal processing techniques for system identification can assist in identifying such network topology changes, faults and line outages. Our goal in this paper is to design algorithms to identify single line outage network topology changes in near real time.

### 1.1 The Setting and Our Contributions

We propose the use of state-estimation based sequential hypothesis testing to detect single line outages. For a given power grid with $n$ links, each link outage is a hypothesis $h_i$ where $i \in \{1, 2, \ldots, n\}$ along with the hypothesis $h_0$ referring to the situation with no link outages. We consider a nonlinear power flow model with power flow measurements, and treat phase angles and voltages as hidden states. We assume that the measurements are such that the power system is "observable" under any single line outage; see subsection 1.2 for a description of the notion of observability.

Our contributions can be summarized as follows.

1. We propose a generalized log-likelihood ratio statistic in a sequential hypothesis testing procedure. The measurements are received at regular time intervals (say 1 second). At each time instant, the central operator processes the received information and either declares that a particular line is in outage (or none is in outage) or proceeds to gather more data before a declaration. We thus have a stopping problem that gathers as much data as needed before a declaration. The decision to stop is based on a fixed and predetermined threshold set to meet a given false detection constraint. The main challenge here is to set the threshold at an

appropriate level that keeps the detection delay small subject to meeting the given false detection constraint.

2. Keeping in mind the communication limitations under centralized operation, we also propose a decentralized dynamic state estimation method using the so-called Unscented Kalman Filter (UKF) [22, 32, 36] to perform a multi-area state estimation followed by line outage identification. Again a generalized likelihood ratio testing procedure, similar to the centralized setting but this time with data aggregated over regions, is used to identify the particular line in outage (if there is one). The main challenges here are to identify the computations that can be delegated to the edge and intermediate nodes and those that need to be retained by the system operator, without affecting the ability to detect single line outages, in addition to setting an appropriate threshold that keeps the detection delay small subject to the false detection constraint, as before.

3. We then test our proposed algorithms on the IEEE 14 bus and the IEEE 118 bus transmission line test systems to demonstrate their validity. Performance study outcomes are provided in the simulations section.

## 1.2 Related Works and Placement of Our Contributions

We first begin with some remarks on observability. Dynamic state estimation tracks the current state of the system (see the textbook [21]). Accurate state estimation requires sufficient measurements from a suitable set of locations [1]. If a set of measurements are sufficient to make state estimation possible, then we say that the power system is observable. Meters are usually placed at appropriate locations to ensure observability [35]. But if observability is not ensured either additional measurements are advised or pseudo-measurements, which are derived from historical data, should be used to obtain good estimates [6]. In this paper we assume that the measurements are such that the power system is observable under any single line outage.

Our proposal involves the use of state estimation for line outage detection. This idea is not new. The topology of the power system is suspected whenever the measurements associated with a transmission line or a bus are flagged as outliers by a state estimation based residual test. A technique for computing indices which quantify the degree of correlation between the estimated quantities and those likely to occur under configuration errors is presented in [9]. The use of normalized residuals obtained from state estimation procedures for the purpose of detection of topology errors is proposed in [34]. The reference [19] proposed a method to detect the network model by comparing state estimation results without topological errors and with topological errors. Topology determination using least absolute value state estimation is presented in [26].

Further, the works [2, 7, 8] have proposed various other techniques to detect and identify topology errors. A method for detection of topology errors within an "unobservable" portion of the system was proposed in [2], while [8] presented a normalized Lagrange multipliers technique. A geometric interpretation of the residual error is provided in [7] which is then used to identify topology errors in power system. The reference [18] proposed a preprocessing method for detecting and identifying topology errors

and bad data measurements prior to doing state estimation. A robust Huber preprocessing method based on a new state estimation model is proposed in [20]. Since the development of PMUs, over the conventional power measurements, recent studies have used phase angle measurements to detect and identify line outages [12, 28, 37] based on the difference between the phase angles of PMU measurements obtained before and after the outage, to identify line outage via hypothesis testing [28], sparse vector estimation [37], or mixed integer nonlinear optimization [12].

The aforementioned works rely on only the current sample and (in some methods) the immediately preceding sample, and do not exploit the fact that once a line outage occurs, outage persists until the line is brought back into service. In this work we use persistence of line outages to our advantage to enable reliable detection.

Our proposed methods use sequential hypothesis testing (see, for e.g., the classic [4]) to identify single line outages. Closest to our work is [3] which proposed a method to detect and identify transmission line outage assuming only phase angle measurements from PMUs (based on a DC approximation model of a power system) and by using the theory of quickest change detection. The DC approximation model is known to be a coarse model. In this work, we look at a finer nonlinear model of the power measurements and treat phase angles and voltages as hidden states. This forces us to deal with nonlinearity of the power measurements in the states, for which a modified approach is needed, in return for much fewer measurements.

The need of both fast and accurate state estimation techniques for wide area monitoring, protection and control is highlighted in [29]. But the distributed nature of the measurement devices poses the communication challenge of transfer of large amounts of state and measurement vector data to a central operator. Numerous multi-area based state estimation techniques have therefore been proposed in [17, 25, 27, 33], where the entire power system is divided into smaller nonoverlapping areas with each area containing its own local operator processing all its local measurements. These are then harmonized with data from neighboring areas. A decentralized dynamic state estimation method using the Unscented Kalman Filter (UKF) was proposed in [36].

In our work, we use a version of the UKF proposed in [22, 32] to perform multi-area state estimation. But our work differs from [22, 32, 36] in that the estimations, based on data aggregated over regions, are but a step leading to the generalized likelihood ratio testing (GLRT) procedure for identifying the particular line in outage (if there is one). The UKF based local procedure has the added advantage of eliminating the need for the measurement Jacobian at the central operator. This significantly reduces not only the communication overhead but also a computational overhead. However, the optimality of the proposed GLRT method for line outage detection needs further investigation.

## 2 MODEL DESCRIPTION

A power system will be represented as a graph $\mathcal{G} = (\mathcal{V}, \mathcal{E})$, where $\mathcal{V}$ is set of buses (or nodes) and $\mathcal{E}$ is the set of links (or branches). Suppose $N = |\mathcal{V}|$ and $n = |\mathcal{E}|$ represent the number of buses and links, respectively. If one of the links $i \in \mathcal{E}$ went down, the information about its effect on the power system will embedded in the

state estimates. By efficiently using this information we can infer the graph of the power system.

Let $\mathcal{H} \in \{\hbar_0, \hbar_1, \hbar_2, \ldots, \hbar_n\}$ denotes the set of hypothesis, where $\hbar_0$ denotes the network with none of the links down, $\hbar_1$ denotes the network with only the first link down, etc. There are $n + 1$ possible hypothesis for the given network. Next we present centralized and decentralized state estimation approaches on an approximate linear model of the power system, with measurements being nonlinear functions of the system state, which will lead us to our eventual goal of state estimation based topology identification.

## 3 CENTRALIZED STATE ESTIMATION

### 3.1 State and Measurements Models

For ease of reference, we provide a list of notations used just before the list of references.

Suppose there are $N$ buses in the system. Suppose that $\theta_{i;t}$ and $V_{i;t}$ are the phase angle and voltage, respectively, at the bus $i$ at time $t$. Then state $x_t$ of the power system at time $t$ is taken to be

$$x_t = [\theta_{1;t}, \theta_{2;t}, \ldots, \theta_{N;t}, V_{1;t}, V_{2;t}, \ldots, V_{N;t}]^T. \tag{1}$$

(Usually the first bus of the system is taken to be the slack bus for which the phase angle $\theta_{1;t}$ is taken as 0, and hence the number of state variables is $2N - 1$. We will however continue to view the state as in $2N$-dimension). We consider a simple approximate linear model for the time evolution of the system state as in [10]. This model states that the state at time $t + 1$ will be same as the state at time $t$, except for some uncertainty which is represented by a random variable. This model is represented by

$$x_{t+1} = x_t + \xi_t \tag{2}$$

where $\xi_t$ is a zero mean Gaussian noise vector with covariance matrix $Q_t$ and $x_t$ is $2N \times 1$ vector of state variables. Suppose there are $M$ measurements $z_t = [z_{1;t}, z_{2;t}, \ldots, z_{M;t}]^T$ obtained at time $t$ from various parts of the system. Usually these measurements consist of power injections at the buses, power flows through the lines, and voltage magnitudes. Instead of using PMUs, we assume that power measurements are available, and voltage (root-mean-square) magnitudes are available but only at power generation buses. These measurements are considered to be the standard set of measurements for state estimation. The measurements and state variables are related through a nonlinear function plus the measurement noise. This relationship can be expressed as

$$z_t = h(x_t) + \psi_t \tag{3}$$

where $\psi_t$ is zero mean Gaussian noise and $h(x_t)$ is $M \times 1$ vector of nonlinear functions. Using the Taylor series to linearize these equations around the previous operating point $x_{t-1}$, and by using $\Delta z_t = z_t - h(x_{t-1})$, the measurement model becomes

$$\Delta z_t = H_{t-1}\Delta x_t + \eta_t, \tag{4}$$

where $\Delta x_t = x_t - x_{t-1}$ and $H_{t-1} = H(x_{t-1})$ is the measurement Jacobian matrix. Construction of measurement Jacobian is explained in [21]. The term $\eta_t$ contains both linearization error and measurement noise. Yet $\eta_t$ is assumed to be zero mean Gaussian noise vector, a common assumption in power systems analysis, with covariance matrix $R_t$. These models are used together for state estimation in power systems. In addition, non-Gaussianity in errors can also

arise due to outlier mechanisms in measurements. Such outliers are usually filtered out in a data clean-up step. See the books [21] and [15]. Note that $h$ without any subscript is used to denote the measurement function and $\hbar_i$ with subscript $i$ is used to denote a hypothesis.

### 3.2 State Estimation

The Kalman filter is a recursive algorithm that can be used in an online estimation framework. The Kalman filtering estimation algorithm consists of two steps: prediction and correction. In the prediction step, it predicts the state and covariance matrix. In next step, it updates the so-called Kalman gain, the state estimate and the covariance matrix. Given eq. (2), the state will be predicted by taking the previous state of the system. We then have the following standard prediction and correction rules.

**Prediction :**

$$x_{t|t-1} = \hat{x}_{t-1|t-1} \tag{5}$$

$$\Sigma_{t|t-1} = \Sigma_{t-1|t-1} + Q_{t-1} \tag{6}$$

**Correction :**

$$K_{t+1} = \Sigma_{t|t-1}H_{t-1}^T \Omega_{t|t-1}^{-1} \tag{7}$$

$$\Omega_{t|t-1} = H_{t-1}\Sigma_{t|t-1}H_{t-1}^T + R_t \tag{8}$$

$$\hat{x}_{t|t} = x_{t|t-1} + K_{t+1}[z_t - H_{t-1}x_{t|t-1}] \tag{9}$$

$$\Sigma_{t|t} = [I - K_{t+1}H_{t-1}]\Sigma_{t|t-1} \tag{10}$$

where

$$x_{t|t-1} = \mathbb{E}[x_t | z^{t-1}]$$

$$\Sigma_{t|t-1} = \mathbb{E}[(x_t - x_{t|t-1})(x_t - x_{t|t-1})^T | z^{t-1}]$$

$$z_{t|t-1} = \mathbb{E}[z_t | z^{t-1}]$$

$$\Omega_{t|t-1} = \mathbb{E}[(z_t - z_{t|t-1})(z_t - z_{t|t-1})^T | z^{t-1}]$$

$$z^{t-1} = (z_0, z_1, \ldots, z_{t-1})$$

and $I$ is the identity matrix of appropriate order.

### 3.3 State Estimation Under Outage

Suppose that the outage occurred at link $i$. We call the resulting network configuration hypothesis as $\hbar_i$. The state evolution equation and the measurement model under the hypothesis $\hbar_i$ become

$$x_{t+1}(\hbar_i) = x_t(\hbar_i) + \xi_t \tag{11}$$

$$\Delta z_t = H_{t-1}(\hbar_i)\Delta x_t(\hbar_i) + \eta_t \tag{12}$$

where $H_{t-1}(\hbar_i)$ is the measurement Jacobian matrix under the hypothesis $\hbar_i$, $\Delta z_t(\hbar_i) = z_t - h(x_{t-1}(\hbar_i))$ and $\Delta x_t(\hbar_i) = x_t(\hbar_i) - x_{t-1}(\hbar_i)$. We assume that $Q_t, R_t$ do not depend on the configuration. (If they do, this can be easily incorporated into the equations.)

Now the Kalman filtering equations for prediction and the correction under the hypothesis $\hbar_i$ can be written analogously as

**Prediction :**

$$x_{t|t-1}(\hbar_i) = \hat{x}_{t-1|t-1}(\hbar_i) \tag{13}$$

$$\Sigma_{t|t-1}(\hbar_i) = \Sigma_{t-1|t-1}(\hbar_i) + Q_{t-1} \tag{14}$$

**Correction :**

$$K_{t+1}(h_i) = \Sigma_{t|t-1}(h_i)H_{t-1}^T(h_i)\Omega_{t|t-1}^{-1}(h_i) \tag{15}$$

$$\Omega_{t|t-1}(h_i) = H_{t-1}(h_i)\Sigma_{t|t-1}(h_i)H_{t-1}^T(h_i) + R_t \tag{16}$$

$$\hat{x}_{t|t}(h_i) = x_{t|t-1}(h_i) + K_{t+1}(h_i)[z_t - H_{t-1}(h_i)x_{t|t-1}(h_i)] \tag{17}$$

$$\Sigma_{t|t}(h_i) = [I - K_{t+1}(h_i)H_{t-1}(h_i)]\Sigma_{t|t-1}(h_i). \tag{18}$$

Before we describe the topology identification method, we quickly describe the decentralized method as well.

## 4 DECENTRALIZED STATE ESTIMATION

Future power systems are likely to have much more buses and lines than today's systems. Performing state estimation at a central location requires that much more communication and computational resources. Instead, if the power system can be divided into multiple subareas, then local state estimation followed by transfer of only aggregated information to the central location will reduce the communication and computational complexity. Assume that the power system is divided into $L$ number of nonoverlapping areas. Individual areas are connected to each other by tie lines across boundary buses, i.e., buses that have lines going out of the area. Each area contains its own set of measurements to run its local state estimation. An unscented Kalman filter (UKF), to be described soon, is used for local state estimation, but there will be disagreement at the boundary buses due to lack of sufficient information to get globally consistent local estimates. A consensus algorithm as explained in [22] is then used to obtain the final estimates. We now provide the details.

### 4.1 State and Measurement Models

Assume that the power system is divided into $L$ number of nonoverlapping areas. The local state vector in area $j \in \{1, 2, \ldots, L\}$ at time step $t + 1$, is a simple linear discrete time transition of states given by

$$x_{j;t+1} = x_{j;t} + \xi_{j;t}, \tag{19}$$

where $x_{j;t}$ is the local state vector of area $j$ at time $t$ and consists of voltage magnitudes and phase angle of all the buses in the area $j$. The vector $\xi_{j;t} \sim N(0, Q_{j;t})$ is white Gaussian noise with zero mean and covariance matrix $Q_{j;t}$ at time step $t$. The measurement model for each area $j$ at time $t$ can be expressed as

$$z_{j;t} = h_j(x_{j;t}) + \eta_{j;t} \tag{20}$$

where $h_j(x_{j;t})$ is the $j$th area's nonlinear function of local state variables $x_{j;t}$, and $\eta_{j;t} \sim N(0, R_{j;t})$ is the white Gaussian noise with mean zero and covariance matrix $R_{j;t}$. Unlike the centralized Kalman filter approach, the UKF avoids the Jacobian matrix as explained below.

### 4.2 UKF State Estimation

Suppose the state vector $x_{j;t-1}$ at time step $t - 1$ and covariance matrix $\Sigma_{j;t-1}$ are known. Let $N_j$ be the number of buses and let $2N_j$ be the dimension of state vector in the area $j$. Set weight factors $\{W_{mj}^{(l)}\}_{l=0}^{4N_j}$ and $\{W_{cj}^{(l)}\}_{l=0}^{4N_j}$ whose use is explained below. The subscript $m$ stands for mean and subscript $c$ stands for covariance. The decentralized UKF is performed in four steps.

Step 1 : Generate $4N_j + 1$ of the so-called *sigma* points $\{X_{j;t-1}^{(l)}\}_{l=0}^{4N_j}$

using $x_{j;t-1}$ and $\Sigma_{j;t-1}$. See Appendix A.

Step 2 : Kalman filter state prediction is done as follows:

$$x_{j;t}^- = \sum_{l=0}^{4N_j} W_{mj}^{(l)} X_{j;t-1}^{(l)} \tag{21}$$

$$\Sigma_{j;t}^- = \sum_{l=0}^{4N_j} W_{cj}^{(l)}[(X_{j;t-1}^{(l)} - x_{j;t}^-)(X_{j;t-1}^{(l)} - x_{j;t}^-)^T] + Q_{j;t-1}. \tag{22}$$

Step 3 : Kalman filter state correction is done as follows.

Generate $4N_j + 1$ sigma points $\{X_{j;t-1}^{-(l)}\}_{l=0}^{4N_j}$ using $x_{j;t}^-$ and $\Sigma_{j;t}^-$, and propagate them through measurement update function

$$z_{j;t}^{-(l)} = h_j(X_{j;t}^{-(l)}). \tag{23}$$

Prediction mean $\mu_{j;t}$, covariance $\Omega_{j;t}$ and cross covariance $C_{j;t}$ of the measurements are obtained by

$$\mu_{j;t} = \sum_{l=0}^{4N_j} W_{mj}^{(l)} z_{j;t}^{-(l)} \tag{24}$$

$$\Omega_{j;t} = \sum_{l=0}^{4N_j} W_{cj}^{(l)}[(z_{j;t}^{-(l)} - \mu_{i;t})(z_{j;t}^{-(l)} - \mu_{i;t})^T] + R_{j;t} \tag{25}$$

$$C_{j;t} = \sum_{l=0}^{4N_j} W_{cl}^{(l)}[(x_{j;t}^{-(l)} - x_{j;t}^-)(z_{j;t}^{-(l)} - \mu_{i;t})^T]. \tag{26}$$

Now calculate the filter gain $K_{j;t}$, state update $\hat{x}_{j;t}$ and covariance $\hat{\Sigma}_{j;t}$ using the equations

$$K_{j;t} = C_{j;t}\Omega_{j;t}^{-1} \tag{27}$$

$$\hat{x}_{j;t} = x_{j;t}^- + K_{j;t}[z_{j;t} - \mu_{j;t}] \tag{28}$$

$$\hat{\Sigma}_{j;t} = \Sigma_{j;t}^- - K_{j;t}\Omega_{j;t}K_{j;t}^T. \tag{29}$$

Each area will perform the above steps independently, but there will be disagreements at boundary buses and external buses over tie lines. All the areas need to communicate with their neighbors across the tie lines because the measurements within a local area are in general insufficient to obtain globally consistent state estimates. A consensus algorithm explained in Step 4, is then used to obtain a consistent state estimate $\tilde{x}_{j;t}$ and covariance $\tilde{\Sigma}_{j;t}$. These feed the UKF for the next iteration. We now briefly discuss the consensus algorithm.

Step 4 : A review of the max- and min-consensus algorithm.

The max- and min-consensus algorithms' goals are to provide interaction rules that specify the information exchange between one area and all its neighbors. Based on $\hat{x}_{j;t}$ and $\hat{\Sigma}_{j;t}$, an ellipsoid is constructed for each area. The idea is that the intersection of these ellipsoids contains the true estimates of the boundary buses. A local set is defined as the smallest axes-aligned box bounding each area ellipsoid. Each area, say $j$, processes its own measurements $z_{j;t}$ to obtain a local set. The global set must lie inside the intersection of the all these local sets. The global set can be computed by exchanging maximum and minimum quantities between neighboring areas. The minimum point of a global set can be computed by using the min-consensus algorithm and maximum point of a global set can be computed by the max-consensus algorithm. See [22] for the detailed min- and max-consensus algorithms.

At each iteration, each area $j$ updates its own shared bus states using the shared bus states of the neighboring areas. While performing the max-consensus algorithm, area $j$ compares its shared bus states to those of its neighbors and always keeps the maximum value. In max-consensus algorithm each shared bus value converges to the maximum value $\zeta_{j;t}^d(+)$ ('+' for maximum) among all its neighbors, where $d$ denotes the $d$th shared bus. Similarly, the min-consensus algorithm converges to the minimum $\zeta_{j;t}^d(-)$ ('−' for minimum).

After performing max- and min-consensus algorithm, a new axes-aligned box is obtained for each area $j$. For each area, the box is bounded by another ellipsoid by minimizing the volume of the ellipsoid. The center of the ellipsoid $\tilde{x}_{j;t}$ and diagonal entries of the associated matrix can be computed by

$$\tilde{x}_{j;t} = \{\tilde{x}_{j;t}^d := (\zeta_{j;t}^d(+) + \zeta_{j;t}^d(-))/2\}_{d=1}^{2N_j} \qquad (30)$$

$$\tilde{\Sigma}_{j;t}^{d;d} = (\zeta_{j;t}^d(+) - \zeta_{j;t}^d(-))^2/2. \qquad (31)$$

The UKF is performed again by using $\tilde{x}_{j;t}$ and $\tilde{\Sigma}_{j;t}$ instead of $x_{j;t}$ and $\Sigma_{j;t}$, respectively. Finally the new $x_{j;t}$ and $\Sigma_{j;t}$ are used in the next iteration for the filtering process. See [22] for details.

### 4.3 State Estimation Under Outage

Even though the state estimation procedure outlined above is decentralized, topology identification requires a central operator to make the final decision. Each area performs a state estimation procedure for each hypothesis $\hbar_i$. Note that the consensus algorithm will require each area to maintain state estimates for all hypothesis including those that are for line outages outside the area. The measurement model under hypothesis $\hbar_i$ can be written as

$$x_{j;t+1}(\hbar_i) = x_{j;t}(\hbar_i) + \xi_{j;t} \qquad (32)$$

$$z_{j;t} = (h_j(x_{j;t}))(\hbar_i) + \eta_{j;t}. \qquad (33)$$

Then, the filtering equations become

$$K_{j;t}(\hbar_i) = C_{j;t}(\hbar_i)\Omega_{j;t}^{-1}(\hbar_i) \qquad (34)$$

$$\Omega_{j;t}(\hbar_i) = \sum_{l=0}^{2n_j} W_{cj}^{(l)}[(z_{j;t}^{-(l)}(\hbar_i) - \mu_{i;t}(\hbar_i))(z_{j;t}^{-(l)}(\hbar_i) - \mu_{i;t}(\hbar_i))^T]$$
$$+ R_{j;t} \qquad (35)$$

$$\hat{x}_{j;t}(\hbar_i) = x_{j;t}(\hbar_i)^- + K_{j;t}(\hbar_i)[z_{j;t} - \mu_{j;t}(\hbar_i)] \qquad (36)$$

$$\hat{\Sigma}_{j;t}(\hbar_i) = \Sigma_{j;t}(\hbar_i)^- - K_{j;t}(\hbar_i)\Omega_{j;t}(\hbar_i)K_{j;t}^T(\hbar_i). \qquad (37)$$

After each area performs its local state estimation, a consensus algorithm [22] computes global estimates, one for each hypothesis. Once the complete estimation is performed each area transfers its local covariance $\Omega_{j;k}(\hbar_i)$ and measurement error $e_{j;t}(\hbar_i) = z_{j;t}(\hbar_i) - \mu_{j;t}(\hbar_i)$ to the central operator. The central operator will use this information to infer outages. We describe the decentralized state estimation based topology inference in section 5.2. Let us note in passing that the state estimation procedure need not converge and yet can be used for sequential hypothesis testing and line outage identification.

## 5 IDENTIFICATION OF LINE OUTAGES USING SEQUENTIAL HYPOTHESIS TESTING

We assume a known initial state $x_0$. A sequential hypothesis testing using log-likelihood ratio is used to identify line outages (hypothesis $\hbar_i$ for outage in line $i$). The log-likelihood ratio at time $t$ can be expressed as

$$\mathcal{Z}_{\hbar_i\hbar_j}^t = \sum_{k=1}^t \log \frac{\mathcal{P}_{\hbar_i}(z_k|z^{k-1})}{\mathcal{P}_{\hbar_j}(z_k|z^{k-1})}, \qquad (38)$$

where $\mathcal{P}_{\hbar_i}(z_k|z^{k-1})$ is the probability of observing measurement $z_k$ at time $k$ under to hypothesis $\hbar_i$ and given the past observations. This equation 38 utilizes the information from previous samples. Hence, any persistence in outage will be detected. Assuming that the state-observation system is Gaussian, i.e., $x_0$ is fixed and $\xi_t, \eta_t$ are iid Gaussian with mean 0 and covariance matrices $Q_t$ and $R_t$ respectively, we have

$$\mathcal{P}_{\hbar_i}(z_k|z^{k-1}) \sim N(z_{k|k-1}, \Omega_{k|k-1}(\hbar_i)).$$

Then, the log-likelihood ratio becomes

$$\mathcal{Z}_{\hbar_i\hbar_j}^t = \frac{1}{2}\sum_{k=1}^t \log \frac{|\Omega_{k|k-1}(\hbar_j)|}{|\Omega_{k|k-1}(\hbar_i)|}$$
$$+ e_k(\hbar_j)^T\Omega_{k|k-1}^{-1}(\hbar_j)e_k(\hbar_j) - e_k(\hbar_i)^T\Omega_{k|k-1}^{-1}(\hbar_i)e_k(\hbar_i)$$
$$(39)$$

where $e_k(\hbar_i) = z_k(\hbar_i) - H_{k-1}(\hbar_i)x_{k|k-1}(\hbar_i)$ is the measurement error under the hypothesis $\hbar_i$. Let

$$\mathcal{Z}_{\hbar}^t = \min_{\hbar' \neq \hbar} \mathcal{Z}_{\hbar\hbar'}^t \qquad (40)$$

denote the log-likelihood ratio of hypothesis $\hbar$ with respect to its *nearest alternative* $\hbar'$ among $\{\hbar_0, \hbar_1, \ldots, \hbar_n\}$. Our proposal for the candidate decision $\hat{\hbar}_t$ at the time $t$ is

$$\hat{\hbar}_t = \arg\max_{\hbar} \mathcal{Z}_{\hbar}^t. \qquad (41)$$

Suppose $\hbar$ is the true hypothesis. We would like

$$P_{\hbar}[\hat{\hbar}_t \neq \hbar] \leq \epsilon, \qquad (42)$$

i.e., the probability that the decision is incorrect is small. As done in [31], this tolerance criterion is attained when

$$\max \mathcal{Z}_{\hat{\hbar}_t}^t \geq \log(\frac{n+1}{\epsilon}), \qquad (43)$$

where $n$ is the number of links in the power system. The central operator can stop and declare $\hat{\hbar}_t$ if eq. (43) holds at time $t$. If eq. (43) does not hold, the central operator continues to sample and continues with the estimation. This ensures that at the time of stoppage and declaration, eq. (42) holds and thus the probability of error is within the tolerance limit.

We now apply this to the power system. The point is, if these is an outage, the measurements will reflect those changes as explained in [4]. By performing sequential hypothesis testing, state estimation tries to fit those measurements to all possible line outage cases and tries to find the best fit topology. Naturally this can be used for identifying more than single line outages, although we have focused only on early detection of single line outages.

## 5.1 Line Outage Detection Using Centralized State Estimation

Suppose that the measurement samples are received at the central location once in every second. Let us assume that an outage has already occurred before time 0. Using the measurement sample received, the Kalman filter performs state estimation and gives the covariance matrix $\Omega_{t|t-1}(\hbar_i)$ and measurement error $e_t(\hbar_i)$ at time $t$. This is done for all hypothesis $\hbar_i$, $i \in \{0, 2, \ldots, n\}$. Then, we use the Equations (39) to (41) to find $\hat{\hbar}_t$. If eq. (43) is satisfied, stop and declare $\hat{\hbar}_t$ as the decision. Otherwise go to next sample to gather more information about line outage.

*Computational complexity.* A straightforward complexity calculation indicates that the complexity of our proposed centralized algorithm is, at each time step, $O(nN(N+M)^2)$ with a small constant multiplier. This is because, at each time and for each hypothesis, the correction step involves triple matrix multiplications and a matrix inversion. These involve $O(N(N+M)^2)$ calculations. With similar calculations involving $n+1$ hypotheses, we see the $O(nN(N+M)^2)$ complexity. The actual likelihood ratio computations (39) and the minimization in (40) are of lower order complexity. This raises a very interesting question of faster Kalman filter updates. There has been some recent interest in reduced complexity Kalman filtering; see for example [23]. The problem of reducing this further or a study of optimality are interesting future directions. See Appendix B.1 for a pseudocode of the algorithm.

## 5.2 Line Outage Detection Using Decentralized State Estimation

In the centralized setting, the central operator has access to all measurements. But only the centralized analogs of $\Omega_{k|k-1}(h_i)$ and $e_t(h_i)$ are required for every $k$ and every $h_i$. These are exactly what we have computed and have made available to the central operator in the decentralized case as well, with only a notation change. Suppose there are $L$ number of areas. Then the covariance matrix and measurement error for hypothesis $\hbar_i$ are obtained as shown below:

$$\Omega_t(\hbar_i) = \begin{bmatrix} \Omega_{1;t}(\hbar_i) & 0 & \cdots & 0 \\ 0 & \Omega_{2;t}(\hbar_i) & \cdots & \vdots \\ \vdots & \vdots & \ddots & 0 \\ 0 & \cdots & 0 & \Omega_{L;t}(\hbar_i) \end{bmatrix} \quad (44)$$

$$e_t(\hbar_i) = [e_{1;t}(\hbar_i), e_{2;t}(\hbar_i), \ldots, e_{L;t}(\hbar_i)]^T,$$

where $\Omega_{l;t}(\hbar_i)$ is as in eq. (25) for hypothesis $\hbar_i$ on area $l$ at time $t$. Note that the covariance matrix is assumed to be block diagonal. This assumption is valid because the error vector blocks come from measurement errors in different blocks each of which represents a different geographical location. We then calculate the log-likelihood ratio at time $t$ using

$$\mathcal{Z}_{\hbar_i \hbar_j}^t = \frac{1}{2} \sum_{k=1}^{t} \log \frac{|\Omega_k(\hbar_j)|}{|\Omega_k(\hbar_i)|} \\ + e_k(\hbar_j)^T \Omega_k^{-1}(\hbar_j) e_k(\hbar_j) - e_k(\hbar_i)^T \Omega_k^{-1}(\hbar_i) e_k(\hbar_i) \ . \quad (45)$$

We then use the Equations (39) to (41) to find $\hat{\hbar}_t$. If eq. (43) is satisfied, declare $\hat{\hbar}_t$ as the decision, otherwise proceed to the next measurement sample. Repeat this procedure until eq. (43) is satisfied.

*Computational complexity.* The computational complexity per regional update is $O(N_j(N_j + M_j)^2)$. Summing this across all regions we get $O(\sum_j N_j(N_j + M_j)^2)$. The consensus algorithms are of lower order complexity. Multiplying the above by the number of hypotheses $n+1$, we see that the complexity is $O(n(\sum_j N_j(N_j + M_j)^2))$. See Appendix B.2 for a pseudocode of the algorithm.

## 6 SIMULATION RESULTS

We test our proposed topology identification algorithm on the IEEE 14 and the IEEE 118 bus systems. We assume that all measurements arrive at the same time without delays. Measurement samples are generated for the respective test systems using normalized daily load profile of Bengaluru, a large metropolitan city in south India. Load variations are introduced at each bus of the test system according to the normalized load profile. Load data contains a 24 hour load profile on a per hour basis. MATLAB curve fitting tools then provide a per second load profile. The measurements considered are power injections at the buses, power flows in the transmission lines and voltage magnitudes at specific buses (as indicated earlier). These were generated for all possible cases of line outages, by solving the power flow equations using the MatPower toolbox in MATLAB [38]. Transformer outages are not considered as they result in diverged power flow solutions. Locations of measurements were chosen to ensure system observability for both centralized and decentralized cases.

### 6.1 Centralized State Estimation

The initial state for state estimation was taken from the power flow solution of the respective outage case. The initial covariance $\Omega_0(\hbar)$ and $\Omega_{0|0}(\hbar)$ were taken to be diagonal with entries set to $10^{-6}$. Also, the elements of diagonal matrix $Q_t$ were kept constant at $10^{-6}$ during the whole simulation. Errors in measurements of power injections, power flows and voltage magnitudes were added assuming Gaussian distribution with zero mean and standard deviation of 0.1% and 2% of base case voltages and powers respectively.

*6.1.1 The 14 bus system.* We simulated two cases using IEEE 14 bus system shown in Figure 1. First, we assumed that measurements are available at every location. In this case the measurement vector contains all measurements other than phase angles, which constitutes a total of 122 measurements. Second, to make the algorithm more realistic, we assumed measurements are available only at some limited locations, yet preserving observability. This set consists of 42 measurements. Measurement set for the entire day, once in every second was generated on IEEE 14 bus system with all lines in service which is considered as base case. For each line outage case also, the measurement set is generated for use in the hypothesis testing procedure. Note that the measurement locations are same for base case and line outage cases. We used the generated data, generated every second, to perform the topology identification as explained in section 5.1. The algorithm was tested with $\epsilon$ values of 0.1, 0.01 and 0.001. Results for the first case, assuming availability
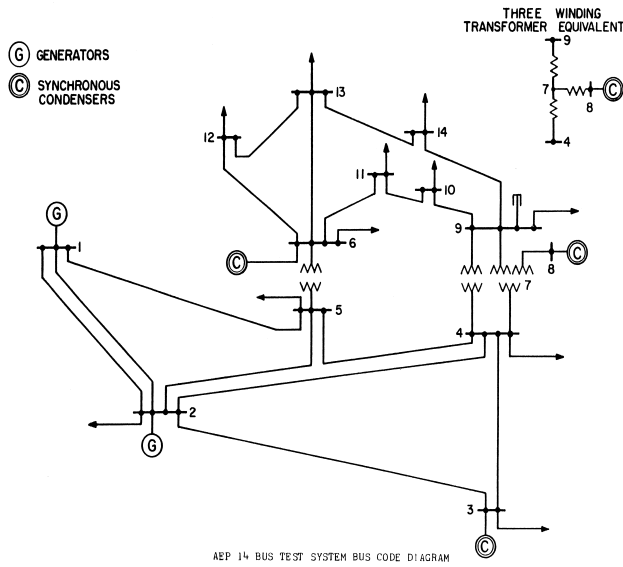
**Figure 1: IEEE 14 Bus Test System**

**Table 1: Simulation results for 14 bus system, assuming all measurements are available except phase angles.**

| Line Outage | $\epsilon$ | False Identification Probability | Average Delay |
| --- | --- | --- | --- |
| 1 - 2 | 0.01 | 0 | 1 |
| 1 - 5 | 0.01 | 0 | 1 |
| 2 - 3 | 0.01 | 0 | 1 |
| 2 - 4 | 0.01 | 0 | 1 |
| 2 - 5 | 0.01 | 0 | 1 |
| 3 - 4 | 0.01 | 0 | 1 |
| 4 - 5 | 0.01 | 0 | 1 |
| 6 - 11 | 0.01 | 0 | 1 |
| 6 - 12 | 0.01 | 0 | 1 |
| 6 - 13 | 0.01 | 0 | 1 |
| 9 - 10 | 0.01 | 0 | 1 |
| 9 - 14 | 0.01 | 0 | 1 |
| 10 - 11 | 0.01 | 0 | 3 |
| 12 - 13 | 0.01 | 0 | 4 |
| 13 - 14 | 0.01 | 0 | 1 |

**Table 2: Simulation results for 14 bus system, assuming only subset of measurements are available.**

| Line Outage | $\epsilon$ | False Identification Probability | Average Delay |
| --- | --- | --- | --- |
| 1 - 2 | 0.01 | 0 | 1 |
| 1 - 5 | 0.01 | 0 | 1 |
| 2 - 3 | 0.01 | 0 | 1 |
| 2 - 4 | 0.01 | 0 | 1 |
| 2 - 5 | 0.01 | 0 | 1 |
| 3 - 4 | 0.01 | 0 | 1 |
| 4 - 5 | 0.01 | 0 | 1 |
| 6 - 11 | 0.01 | 0 | 1 |
| 6 - 12 | 0.01 | 0 | 1 |
| 6 - 13 | 0.01 | 0 | 1 |
| 9 - 10 | 0.01 | 0 | 1 |
| 9 - 14 | 0.01 | 0 | 1 |
| 10 - 11 | 0.01 | 0 | 1 |
| 12 - 13 | 0.01 | 0 | 1 |
| 13 - 14 | 0.01 | 0 | 1 |

of all measurements except phase angles is presented in the Table 1. Results for the second case are presented in Table 2.

The first column in the results indicates the link outage considered in the simulation. The second column represents false identification probability, i.e., how many times the algorithm failed to identify the faulty link for a given value of $\epsilon$. The third column represents average delay (average number of samples) for a decision. For example, in Table 1, in case of hypothesis $h_1$, i.e., when there is outage of the line between buses 1 and 2, the algorithm correctly identified $h_1$ as true every time out of $\frac{100}{\epsilon}$ experiments with an average delay of 1 sample (1 second). For detecting outage of line 12-13, the algorithm took an average 4 samples to make a decision and was correct every time in the $\frac{100}{\epsilon}$ experiments. Similarly, outage of line 10-11 took an average delay of 3 samples for detection. We found that these line outages do not change the resultant power flow appreciably and hence more samples are needed for detection of their outages.

In Table 2 one can observe that average delay turns out to be one sample for all the line outages. For both the tables $\epsilon = 0.01$ was chosen mainly for illustration purposes and quick simulation. One anticipates that the expected time for a decision grows with $\epsilon$ as $\log(1/\epsilon)$ [31].

*6.1.2   The 118 bus system.* The IEEE 118 bus system shown in Figure 2 is used to test the scalability of our proposed algorithm. Simulation results on the IEEE 118 bus system assuming measurements other than phase angles are available at all locations are presented in Table 3. Here the results for top 5 critical line outages, obtained from contingency analysis, are presented. Initializations for 118 bus case are the same as for the 14 bus system. From Table 3 one can observe that outage of the line 88-89 takes longer time to identify. We have chosen $\epsilon = 0.01$ for all the cases.

**Table 3: Simulation results for 118 bus system with centralized state estimation, assuming all measurements are available except phase angles.**

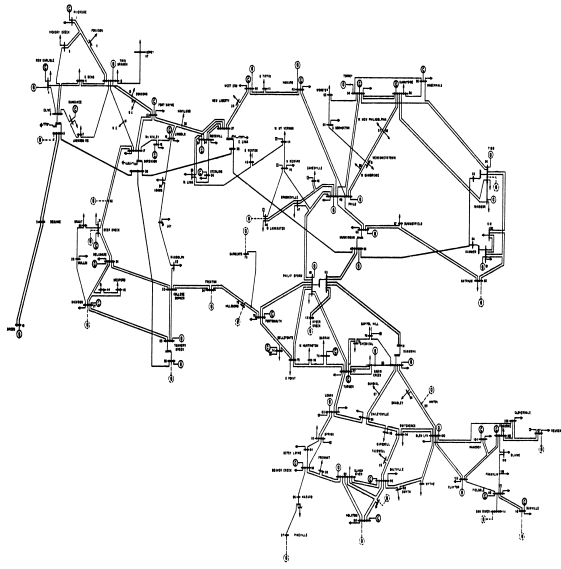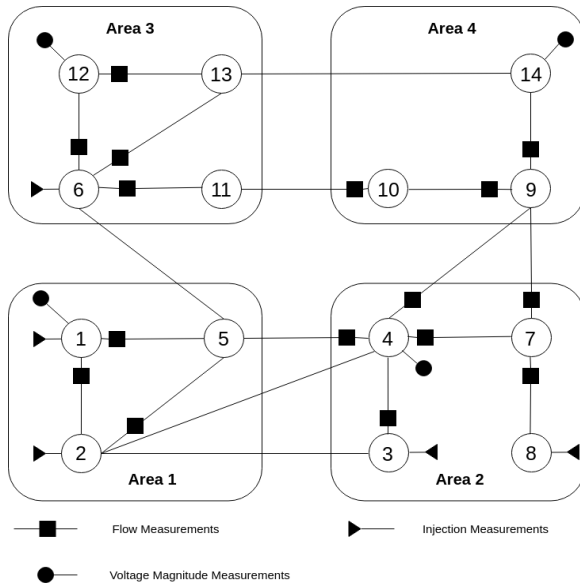| Line Outage | $\epsilon$ | False Identification Probability | Average Delay |
| --- | --- | --- | --- |
| 82 - 83 | 0.01 | 0 | 1 |
| 83 - 85 | 0.01 | 0.01 | 2.16 |
| 89 - 90 | 0.01 | 0 | 1 |
| 85 - 89 | 0.01 | 0 | 1 |
| 88 - 89 | 0.01 | 0 | 4 |

**Figure 2: IEEE 118 Bus Test System**



**Figure 3: IEEE 14 Bus Test System divided into 4 nonoverlapping areas.**

## 6.2 Decentralized State Estimation

In this section we present the results of decentralized state estimation based topology identification method presented in section 5.2.

*6.2.1 The 14 bus system.* The IEEE 14 bus system is divided into 4 nonoverlapping areas as shown in Figure 3. Here we presented two cases: assuming all measurements available and only subset of them available. For the second case measurement locations are

**Table 4: Bus partition of IEEE 14 bus system.**

| Area | Internal buses | Boundary buses | External buses |
|------|----------------|----------------|----------------|
| 1 | 1 | 2,5 | 3,4 |
| 2 | 8 | 3,4,7 | 2,5,9 |
| 3 | 12 | 6,11,13 | 5,14 |
| 4 | 14 | 9,10 | 4,7,11 |

**Table 5: Simulation results for 14 bus system with decentralized state estimation, assuming full set of measurements are available except phase angles.**

| Line Outage | $\epsilon$ | False Identification Probability | Average Delay |
|-------------|------------|----------------------------------|---------------|
| 1 - 2 | 0.01 | 0 | 1 |
| 1 - 5 | 0.01 | 0 | 1 |
| 2 - 3 | 0.001 | 0.774 | 4.153 |
| 2 - 4 | 0.001 | 0 | 1.096 |
| 2 - 5 | 0.01 | 0 | 1 |
| 3 - 4 | 0.01 | 0 | 1 |
| 4 - 5 | 0.001 | 0 | 2.2 |
| 6 - 11 | 0.001 | 0 | 1.841 |
| 6 - 12 | 0.01 | 0 | 1 |
| 6 - 13 | 0.01 | 0 | 1 |
| 9 - 10 | 0.001 | 0 | 2.419 |
| 9 - 14 | 0.01 | 0 | 1 |
| 10 - 11 | 0.001 | 0.74 | 11.75 |
| 12 - 13 | 0.001 | 0 | 2.16 |
| 13 - 14 | 0.001 | 0 | 1.37 |

indicated in Figure 3. Table 4 shows the corresponding bus partitioning. Initializations for the decentralized case are the same as in the centralized case. All areas perform their local estimators and then use the consensus algorithm to obtain global estimates. These are then sent to the central operator. The central operator uses this information to test hypotheses and find line outages. Table 5 and Table 6 provide the simulation results for the 14 bus system in the decentralized setting, with the full set of measurements and with a subset of measurements, respectively.

In both cases line outages at (1-2), (1-5), (2-5), (3-4) and (6-13) are identified very quickly with $\epsilon = 10^{-2}$. However, line outages at (2-4), (4-5), (6-11), (9-10), (12-13) and (13-14) took more than one second to identify with $\epsilon = 10^{-3}$. Every outage case is repeated for $\frac{100}{\epsilon}$ times to check the accuracy for a given $\epsilon$. In many cases, our perfect detection seems to suggest that our choice of $\epsilon$ may be conservative. Even so, our algorithm failed to identify line outages (2-3) and (10-11). As shown in Figure 3 these lines represent the lines between the areas. Outage at these lines causes insufficient flow of information between areas, making state estimation results inaccurate. Work is under progress to see if these could be identified as well.

*6.2.2 The 118 bus system.* The partitioned IEEE 118 bus system is shown in Figure 4. The entire system is divided into 3 nonoverlapping areas. Table 7 contains the partitioning details. Simulation

**Table 6: Simulation results for 14 bus system with decentralized state estimation, assuming only subset of measurements are available.**

| Line Outage | $\epsilon$ | False Identification Probability | Average Delay |
|---|---|---|---|
| 1 - 2 | 0.01 | 0 | 1 |
| 1 - 5 | 0.01 | 0 | 1 |
| 2 - 3 | 0.001 | 0.862 | 8.623 |
| 2 - 4 | 0.001 | 0 | 1.948 |
| 2 - 5 | 0.01 | 0 | 1 |
| 3 - 4 | 0.01 | 0 | 1 |
| 4 - 5 | 0.01 | 0 | 2.32 |
| 6 - 11 | 0.001 | 0 | 2.913 |
| 6 - 12 | 0.001 | 0 | 1.043 |
| 6 - 13 | 0.01 | 0 | 1 |
| 9 - 10 | 0.01 | 0 | 1.8 |
| 9 - 14 | 0.001 | 0 | 1 |
| 10 - 11 | 0.001 | 0.835 | 7.017 |
| 12 - 13 | 0.001 | 0.002 | 2.16 |
| 13 - 14 | 0.001 | 0 | 1.84 |
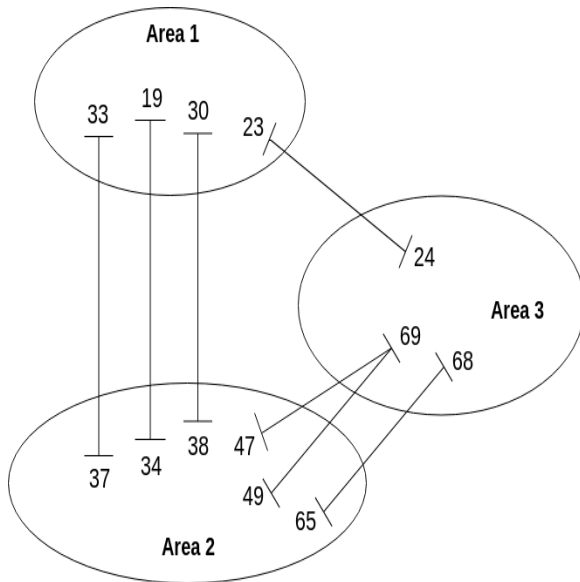


**Figure 4: IEEE 118 Bus Test System divided into 3 nonoverlapping areas.**

**Table 7: Bus partition of IEEE 118 bus system.**

| Area | Internal buses | Boundary buses | External buses |
|---|---|---|---|
| 1 | 1-18, 20-22, 25-29, 31, 32, 113-115, 117 | 19, 23, 30, 33 | 24, 34, 37, 38 |
| 2 | 35, 36, 39-46, 48, 50-64, 66, 67 | 34, 37, 38, 47, 49, 65 | 19, 30, 33, 68, 69 |
| 3 | 70-112, 116, 118 | 24, 68, 69 | 23, 47, 49, 65 |

**Table 8: Simulation results for 118 bus system with decentralized state estimation, assuming all measurements are available except phase angles.**

| Line Outage | $\epsilon$ | False Identification Probability | Average Delay |
|---|---|---|---|
| 82 - 83 | 0.01 | 0 | 1 |
| 83 - 85 | 0.01 | 0 | 1 |
| 89 - 90 | 0.01 | 0 | 1 |
| 85 - 89 | 0.01 | 0 | 1 |
| 88 - 89 | 0.01 | 0 | 5.64 |

results with full measurement set are presented in Table 8. Simulation results for critical line outages are presented with $\epsilon = 10^{-2}$. It can be observed from the table that the line outage 88-89 takes a longer time to identify with an average delay of 5.64 seconds. The decentralized line outage estimation with minimal set of measurements for this system is under progress.

### 6.3 Comparison with a Previous Work

The results of [3] on the more frequently sampled PMU data show that the average detection delay for the 118-bus system varies between 1–2 samples (0.03-0.06 seconds) for some link outages to between 100–150 samples (3-5 seconds) depending on the 'mean time to false alarm' constraint imposed on the policy. Our simulation results indicate that our decentralized algorithm takes between 1 sample (1 second) to 5–6 samples (5.64 seconds) for detecting a line outage, depending on the false identification probability. We thus see that the decentralized algorithm with less frequently sampled power measurements comes close to the performance attained with the more frequently sampled PMU data.

### 7 CONCLUSIONS

In this paper, we presented an approach to identify single line outages by exploiting the statistical properties of state estimation results. We also proposed a decentralized state estimation based line outage detection approach. We assumed that the measurements are obtained once every second and state estimation was performed dynamically. By sequentially processing the information obtained from state estimation, our algorithm was able to identify single line outages within a few samples. As one can see from the simulations, the decentralized algorithm takes a little longer to detect line outage, but has lesser communication and computational overhead.

Even though state estimation is decentralized, line outage detection algorithm is still centralized. In future work we plan to include the design of decentralized line outage detection algorithms to further reduce the computational burden and a design of fully decentralized state estimation algorithms.

### NOMENCLATURE

| | |
|---|---|
| $\epsilon$ | False alarm probability |
| $\eta_t$ | Zero mean Gaussian noise vector of dimension $M \times 1$ |
| $\eta_{j;t}$ | Zero mean Gaussian noise vector |
| $\mathcal{E}$ | Set of links (or branches) |
| $\mathcal{G}$ | Graph representing a power system |

$\hbar_i$      $i$-th hypothesis

$\mathcal{H}$      Set of all possible hypothesis

$\mathcal{P}_{\hbar_i}$      Probability function under hypothesis $\hbar_i$

$\mathcal{V}$      Set of buses (or nodes)

$\mathcal{Z}^t_{\hbar_i \hbar_j}$      Log-likelihood ratio between the hypothesis $\hbar_i$ and $\hbar_j$ at time $t$

$\mu_{j;t}$      Measurement mean in ares $j$ at time $t$

$\Omega_{j;t}$      Measurement error covariance matrix in area $j$ at time $t$

$\Omega_{j;t}(\hbar_i)$      Measurement error covariance matrix in area $j$ at time $t$ under hypothesis $\hbar_i$

$\psi_t$      Zero mean Gaussian noise vector of dimension $M \times 1$

$\Sigma_{j;t}$      State error covariance matrix of area $j$ at time $t$

$\Sigma_{j;t}(\hbar_i)$      State error covariance matrix of area $j$ at time $t$ under hypothesis $\hbar_i$

$\theta_{i;t}$      Phase angle at bus $i$ at time $t$

$\xi_t$      Gaussian noise vector of dimension $2N \times 1$

$\xi_{j;t}$      Zero mean Gaussian noise vector of area $j$ at time $t$ of dimension $2N_j \times 1$

$\{W_{cj}\}^{4N_j}_{l=0}$      Weight factor for calculating covariance in UKF state estimation for area $j$

$\{W_{mj}\}^{4N_j}_{l=0}$      Weight factor for calculating mean in UKF state estimation for area $j$

$\{X^{(l)}_{j;t}\}^{4N_j}_{l=0}$      Sigma points of states for area $j$

$\{z^{-(l)}_{j;t}\}^{4N_j}_{l=0}$      Sigma points of measurements for area $j$

$C_{j;t}$      Cross covariance matrix in area $j$ at time $t$

$C_{j;t}(\hbar_i)$      Cross covariance matrix in area $j$ at time $t$ under hypothesis $\hbar_i$

$e_k(\hbar_i)$      Measurement error at time $t$, under hypothesis $\hbar_i$

$h(x_t)$      Vector of nonlinear functions, with dimension $M \times 1$

$h_j(x_{j;t})$      Vector of nonlinear functions in area $j$ at time $t$

$H_t$      Measurement Jacobian matrix of dimension $M \times 2N$

$H_t(\hbar_i)$      Measurement Jacobian matrix of dimension $M \times 2N$ under the hypothesis $\hbar_i$

$K_t$      Kalman gain at time $t$

$K_t(\hbar_i)$      Kalman filer gain at time $t$ under hypothesis $\hbar_i$

$K_{j;t}$      Kalman gain in area $j$ at time $t$

$K_{j;t}(\hbar_i)$      Kalman gain in area $j$ at time $t$ under hypothesis $\hbar_i$

$M$      Total number of measurements

$N$      Number of buses in a power system

$n$      Number of links

$N_j$      Number of buses in area $j$

$Q_t$      Covariance matrix of a $xi_t$ at time $t$, of dimension $2N \times 2N$

$Q_{j;t}$      Covariance matrix of a $xi_{j;t}$ of area $j$ at time $t$, of dimension $2N_j \times 2N_j$

$R_{j;t}$      Covariance matrix of $\eta_{j;t}$

$V_{i;t}$      Voltage magnitude at bus $i$ at time $t$

$x_t$      State vector at time $t$, of dimension $2N \times 1$

$x_t(\hbar_i)$      State vector at time $t$, under hypothesis $\hbar_i$

$x_{j;t}$      State vector of area $j$ at time $t$ of dimension $2N_j$

$z_t$      Measurement vector at $t$ of dimension $M \times 1$

$z_{j;t}$      Measurement vector of area $j$ at time $t$

## REFERENCES

[1] A. Abur and F. H. Magnago. 1999. Optimal meter placement for maintaining observability during single branch outages. *IEEE Transactions on Power Systems* 14, 4 (Nov 1999), 1273–1278. https://doi.org/10.1109/59.801884

[2] F. L. Alvarado. 1981. Determination of External System Topology Errors. *IEEE Transactions on Power Apparatus and Systems* PAS-100, 11 (Nov 1981), 4553–4561. https://doi.org/10.1109/TPAS.1981.316835

[3] T. Banerjee, Y. C. Chen, A. D. Dominguez-Garcia, and V. V. Veeravalli. 2014. Power system line outage detection and identification — A quickest change detection approach. In *2014 IEEE International Conference on Acoustics, Speech and Signal Processing (ICASSP)*. IEEE, Florence, Italy, 3450–3454. https://doi.org/10.1109/ICASSP.2014.6854241

[4] S.A. Bessler. 1960. *Theory and Applications of the Sequential Design of Experiments, K-actions and Infinitely Many Experiments*. Department of Statistics, Stanford University., California, USA. https://books.google.co.in/books?id=M40UAAAAIAAJ

[5] Central Electricity Regulatory Commission (CERC). 2012. Report on Grid Disturbance On 30th and 31st July 2012. Retrieved January 18, 2019 from http://www.cercind.gov.in/2012/orders/Final_Report_Grid_Disturbance.pdf

[6] K. A. Clements. 2011. The impact of pseudo-measurements on state estimator accuracy. In *2011 IEEE Power and Energy Society General Meeting*. IEEE, San Diego, CA, USA, 1–4. https://doi.org/10.1109/PES.2011.6039370

[7] K. A. Clements and A. S. Costa. 1998. Topology error identification using normalized Lagrange multipliers. *IEEE Transactions on Power Systems* 13, 2 (May 1998), 347–353. https://doi.org/10.1109/59.667350

[8] K. A. Clements and P. W. Davis. 1988. Detection and identification of topology errors in electric power systems. *IEEE Transactions on Power Systems* 3, 4 (Nov 1988), 1748–1753. https://doi.org/10.1109/59.192991

[9] I. S. Costa and J. A. Leao. 1993. Identification of topology errors in power system state estimation. *IEEE Transactions on Power Systems* 8, 4 (Nov 1993), 1531–1538. https://doi.org/10.1109/59.260956

[10] A. S. Debs and R. E. Larson. 1970. A Dynamic Estimator for Tracking the State of a Power System. *IEEE Transactions on Power Apparatus and Systems* PAS-89, 7 (Sep. 1970), 1670–1678. https://doi.org/10.1109/TPAS.1970.292822

[11] P. Dey, R. Mehra, F. Kazi, S. Wagh, and N. M. Singh. 2016. Impact of Topology on the Propagation of Cascading Failure in Power Grid. *IEEE Transactions on Smart Grid* 7, 4 (July 2016), 1970–1978. https://doi.org/10.1109/TSG.2016.2558465

[12] R. Emami and A. Abur. 2013. External system line outage identification using phasor measurement units. *IEEE Transactions on Power Systems* 28, 2 (May 2013), 1035–1040. https://doi.org/10.1109/TPWRS.2012.2220865

[13] FERC and NERC. 2011. Arizona-Southern California outages on September 8, 2011. Retrieved January 18, 2019 from https://www.ferc.gov/legal/staff-reports/04-27-2012-ferc-nerc-report.pdf

[14] U.S.-Canada Power System Outage Task Force. and United States. 2004. *Final report on the August 14, 2003 blackout in the United States and Canada [electronic resource] : causes and recommendations / U.S.-Canada Power System Outage Task Force*. U.S. Dept. of Energy [Washington, D.C, Washington, D.C.

[15] Antonio Gomez-Exposito and Ali Abur. 2004. *Power system state estimation: theory and implementation*. CRC press, New York, USA.

[16] P. D. H. Hines, I. Dobson, and P. Rezaei. 2017. Cascading Power Outages Propagate Locally in an Influence Graph That is Not the Actual Grid Topology. *IEEE Transactions on Power Systems* 32, 2 (March 2017), 958–967. https://doi.org/10.1109/TPWRS.2016.2578259

[17] S. Kar, G. Hug, J. Mohammadi, and J. M. F. Moura. 2014. Distributed State Estimation and Energy Management in Smart Grids: A Consensus +Innovations Approach. *IEEE Journal of Selected Topics in Signal Processing* 8, 6 (Dec 2014), 1022–1038. https://doi.org/10.1109/JSTSP.2014.2364545

[18] Serge Lefebvre and Jacques Prévost. 2006. Topology error detection and identification in network analysis. *International Journal of Electrical Power & Energy Systems* 28, 5 (2006), 293 – 305. https://doi.org/10.1016/j.ijepes.2005.12.006

[19] R. L. Lugtu, D. F. Hackett, K. C. Liu, and D. D. Might. 1980. Power System State Estimation: Detection of Topological Errors. *IEEE Transactions on Power Apparatus and Systems* PAS-99, 6 (Nov 1980), 2406–2412. https://doi.org/10.1109/TPAS.1980.319807

[20] L. Mili, G. Steeno, F. Dobraca, and D. French. 1999. A robust estimation method for topology error identification. *IEEE Transactions on Power Systems* 14, 4 (Nov 1999), 1469–1476. https://doi.org/10.1109/59.801932

[21] A Monticelli. 1999. *State Estimation in Electric Power Systems: A Generalized Approach.* Springer US, New York, US. https://doi.org/10.1007/978-1-4615-4999-4

[22] Xiangyun Qing, Hamid Reza Karimi, Yugang Niu, and Xingyu Wang. 2015. Decentralized unscented Kalman filter based on a consensus algorithm for multi-area dynamic state estimation in power systems. *International Journal of Electrical Power & Energy Systems* 65 (2015), 26 – 33. https://doi.org/10.1016/j.ijepes.2014.09.024

[23] Matti Raitoharju and Robert Piché. 2015. On computational complexity reduction methods for Kalman filter extensions. (2015).

[24] V. Rampurkar, P. Pentayya, H. A. Mangalvedekar, and F. Kazi. 2016. Cascading Failure Analysis for Indian Power Grid. *IEEE Transactions on Smart Grid* 7, 4 (July 2016), 1951–1960. https://doi.org/10.1109/TSG.2016.2530679

[25] A. K. Singh and B. C. Pal. 2014. Decentralized Dynamic State Estimation in Power Systems Using Unscented Transformation. *IEEE Transactions on Power Systems* 29, 2 (March 2014), 794–804. https://doi.org/10.1109/TPWRS.2013.2281323

[26] H. Singh and F. L. Alvarado. 1995. Network topology determination using least absolute value state estimation. *IEEE Transactions on Power Systems* 10, 3 (Aug 1995), 1159–1165. https://doi.org/10.1109/59.466541

[27] X. Tai, Z. Lin, M. Fu, and Y. Sun. 2013. A new distributed state estimation technique for power networks. In *2013 American Control Conference.* IEEE, Washington, DC, USA, 3338–3343. https://doi.org/10.1109/ACC.2013.6580347

[28] J. E. Tate and T. J. Overbye. 2008. Line Outage Detection Using Phasor Angle Measurements. *IEEE Transactions on Power Systems* 23, 4 (Nov 2008), 1644–1652. https://doi.org/10.1109/TPWRS.2008.2004826

[29] V. Terzija, G. Valverde, D. Cai, P. Regulski, V. Madani, J. Fitch, S. Skok, M. M. Begovic, and A. Phadke. 2011. Wide-Area Monitoring, Protection, and Control of Future Electric Power Networks. *Proc. IEEE* 99, 1 (Jan 2011), 80–93. https://doi.org/10.1109/JPROC.2010.2060450

[30] UCTE. 2004. FINAL REPORT of the Investigation Committee on the 28 September 2003 Blackout in Italy. Retrieved February 3, 2019 from http://www.rae.gr/old/cases/C13/italy/UCTE_rept.pdf

[31] N. K. Vaidhiyan and R. Sundaresan. 2018. Learning to Detect an Oddball Target. *IEEE Transactions on Information Theory* 64, 2 (Feb 2018), 831–852. https://doi.org/10.1109/TIT.2017.2778264

[32] G. Valverde and V. Terzija. 2011. Unscented kalman filter for power system dynamic state estimation. *IET Generation, Transmission Distribution* 5, 1 (Jan 2011), 29–37. https://doi.org/10.1049/iet-gtd.2010.0210

[33] C. Wang, Z. Qin, Y. Hou, and J. Yan. 2018. Multi-Area Dynamic State Estimation With PMU Measurements by an Equality Constrained Extended Kalman Filter. *IEEE Transactions on Smart Grid* 9, 2 (March 2018), 900–910.

[34] F. F. Wu and W. E. Liu. 1989. Detection of Topology Errors by State Estimation. *IEEE Power Engineering Review* 9, 2 (Feb 1989), 50–51. https://doi.org/10.1109/MPER.1989.4310474

[35] F. F. Wu and A. Monticelli. 1985. Network Observability: Theory. *IEEE Transactions on Power Apparatus and Systems* PAS-104, 5 (May 1985), 1042–1048. https://doi.org/10.1109/TPAS.1985.323454

[36] J. Zhao and L. Mili. 2018. Power System Robust Decentralized Dynamic State Estimation Based on Multiple Hypothesis Testing. *IEEE Transactions on Power Systems* 33, 4 (July 2018), 4553–4562. https://doi.org/10.1109/TPWRS.2017.2785344

[37] H. Zhu and G. B. Giannakis. 2012. Sparse Overcomplete Representations for Efficient Identification of Power Line Outages. *IEEE Transactions on Power Systems* 27, 4 (Nov 2012), 2215–2224. https://doi.org/10.1109/TPWRS.2012.2192142

[38] R. D. Zimmerman, C. E. Murillo-Sanchez, and R. J. Thomas. 2011. MATPOWER: Steady-State Operations, Planning, and Analysis Tools for Power Systems Research and Education. *IEEE Transactions on Power Systems* 26, 1 (Feb 2011), 12–19. https://doi.org/10.1109/TPWRS.2010.2051168

# A  UNSCENTED TRANSFORMATION

The accuracy of non-linear state estimation heavily depends on the approximation of the non-linear function in the neighborhood of the previous point. If approximation is erroneous, then state estimation will be inaccurate. The idea of Unscented transformation (UT) is based on the principle that it is significantly easier to approximate a Gaussian function than non-linear function. Here we provide the generation of sigma points for each area using UT in our simulations. Let us consider that $x_{j;t}$ is the state of the power system at time $t$ in an area $j$, then power system model can be written as

$$x_{j;t+1} = x_{j;t} + \xi_{j;t} \tag{46}$$

$$z_{j;t} = h(x_{j;t}) + \eta_{j;t} \tag{47}$$

All the variables and notations are described in section 4.2. Now the idea of UT is to generate a set of vectors called sigma points, using state vector $x_{j;t-1}$ and covariance $\Sigma_{j;t-1}$, which are given. Then the sigma points are propagated through the non-linear function $h(x_{j;t})$ to estimate the mean and covariance of $z_{j;t}$.

Let $N_j$ is the number of buses and $2N_j$ is the dimension of state vector in the area $j$. A set of $4N_j + 1$ sigma points are generated by

$$X_{j;t-1}^{(0)} = x_{j;t-1} \tag{48}$$

$$X_{j;t-1}^{(l)} = x_{j;t-1} + \sqrt{(2N_j + \lambda)\Sigma_{j;t-1}}_l, \, l = 1, 2, \ldots, 2N_j \tag{49}$$

$$X_{j;t-1}^{(N_j+l)} = x_{j;t-1} - \sqrt{(2N_j + \lambda)\Sigma_{j;t-1}}_l, \, l = 1, 2, \ldots, 2N_j \tag{50}$$

where $(A)_l$ is the $l$th column of the matrix $A$ and the parameter $\lambda$ is defined as

$$\lambda = \alpha^2(2N_j + \kappa) - 2N_j \tag{51}$$

where $\kappa$ can be $3 - 2N_j$ or 0. The parameter $\kappa$ can be used to reduce the higher order error of the mean and the covariance approximations. For Gaussian distributions it is suggested to use $10^4 \leq \alpha \leq 1$. Sigma points are the vectors whose components contains real numbers. In our simulations, we consider $\kappa = 3 - 2N_j$ and $\alpha = 10^2$.

If $\Sigma_{j;t-1}$ is positive definite matrix, the square root can be approximated by $\Sigma_{j;t-1} = AA^T$, where $A$ is the lower triangular matrix obtained form Cholesky factorization of $\Sigma_{j;t-1}$. By using Cholesky factorization, we can avoid the complex number in sigma points as they are real numbers.

Propagate each sigma point through the non-linear function to obtain propagated sigma points

$$z_{j;t}^{-(l)} = h(X_{j;t}^{-(l)}), \, l = 1, 2, \ldots, 4N_j + 1. \tag{52}$$

The advantage of UT is that the mean and error covariance of the measurements can be determined using propagated sigma points evaluated in eq. (52). Propagated mean $\mu_{j;t}$, covariance $\Omega_{j;t}$ and cross covariance $C_{j;t}$ of the measurements are obtained by

$$\mu_{j;t} = \sum_{l=0}^{4N_j} W_{mj}^{(l)} z_{j;t}^{-(l)} \tag{53}$$

$$\Omega_{j;t} = \sum_{l=0}^{4N_j} W_{cj}^{(l)}[(z_{j;t}^{-(l)} - \mu_{i;t})(z_{j;t}^{-(l)} - \mu_{i;t})^T] \tag{54}$$

$$C_{j;t} = \sum_{l=0}^{4N_j} W_{cl}^{(l)}[(x_{j;t}^{-(l)} - x_{j;t}^-)(z_{j;t}^{-(l)} - \mu_{i;t})^T]. \tag{55}$$

The weight factors in Equations (53) to (55) can be determined using the following formulae

$$W_{mj}^{(0)} = \frac{\lambda}{2N_j + \lambda}, W_{cj}^{(0)} = \frac{\lambda}{2N_j + \lambda} + (1 - \alpha^2 + \beta) \tag{56}$$

$$\{W_{mj}^{(l)}\}_{l=1}^{4N_j} = \{W_{cj}^{(l)}\}_{l=1}^{4N_j} = \frac{1}{2(2N_j + \lambda)} \tag{57}$$

in which, the typical value of $\beta$ can be taken as 2 for Gaussian distributions.

# B PSEUDOCODES

## B.1 Algorithm 1 : Line Outage Identification using Centralized State Estimation

**input** : $z_t$, $n$, $\epsilon$, case-data
**output** : $\hat{h}_t$ (Line under outage)
**Initializations** : $t \leftarrow 0, \hat{h}_t \leftarrow \hbar_0, \text{MAX}\mathcal{Z}^t_{\hat{h}_t} \leftarrow 0$,

$\quad \mathcal{Z}^t_{h_i h_j} \leftarrow O_{n+1 \times n+1}, \mathcal{Z}^{t-1}_{h_i h_j} \leftarrow O_{n+1 \times n+1}$,
$\quad e_{th}$                 // $e_{th} \leftarrow$ Error Threshold

**while** $MAX\mathcal{Z}^t_{\hat{h}_t} < \log(\frac{n+1}{\epsilon})$ **do**

  **for** $i \leftarrow 0$ **to** $n$ **do**

    **Function** CentralizedSE($i,z_t$,case-data):

      $x_{t-1|t-1} \leftarrow$ Obtained by performing the Power Flow Solution using the case-data under $i^{th}$ line outage
      **Initialize** : $\Sigma_{t-1|t-1}, Q_{t-1}, R_t$,
      $\quad \Sigma_{t|t-1} \leftarrow \Sigma_{t-1|t-1} + Q_{t-1}$
      $H_{t-1} \leftarrow$ Compute the Measurement Jacobian using $x_{t|t-1}$
      $e_t \leftarrow z_t - H_{t-1}x_{t|t-1}$
      $error \leftarrow e_t e_t^T$
      **while** $error < e_{th}$ **do**
        $\Omega_{t|t-1} \leftarrow H_{t-1}\Sigma_{t|t-1}H_{t-1}^T + R_t$
        $K_{t+1} \leftarrow \Sigma_{t|t-1}H_{t-1}^T\Omega_{t|t-1}^{-1}$
        $\hat{x}_{t|t} \leftarrow x_{t|t-1} + K_{t+1}[z_t - H_{t-1}x_{t|t-1}]$
        $\Sigma_{t|t} \leftarrow [I - K_{t+1}H_{t-1}]\Sigma_{t|t-1}$
        $H_t \leftarrow$ Update the Jacobian matrix using new $\hat{x}_{t|t}$
        $e_t \leftarrow z_t - H_t\hat{x}_{t|t}$
        $error \leftarrow e_t e_t^T$
        $H_{t-1} \leftarrow H_t, \Sigma_{t|t-1} \leftarrow \Sigma_{t|t}, x_{t|t-1} \leftarrow \hat{x}_{t|t}$
      **end**
      **return** $\Omega_{t|t-1}, e_t$
    **End Function**
    $\Omega\{i\} \leftarrow \Omega_{t|t-1}, e\{i\} \leftarrow e_t$

  **end**

  **for** $i \leftarrow 0$ **to** $n$ **do**
    **for** $j \leftarrow 0$ **to** $n$ **do**
      Compute Elements of $\mathcal{Z}^t_{h_i h_j}$    // Eq. (39)
    **end**
  **end**
  $\mathcal{Z}^t_{h_i h_j} \leftarrow \mathcal{Z}^{t-1}_{h_i h_j} + \mathcal{Z}^t_{h_i h_j}$
  $\mathcal{Z}^t_h \leftarrow \min_{\hbar' \neq \hbar} \mathcal{Z}^t_{\hbar\hbar'}$
  $\text{MAX}\mathcal{Z}^t_{\hat{h}_t} \leftarrow \max_{\hbar}(\mathcal{Z}^t_h)$
  $\hat{h}_t \leftarrow \arg\max_h \mathcal{Z}^t_{\hbar}$
  $t \leftarrow t + 1$
**end**
**return** $\hat{h}_t$

## B.2 Algorithm 2 : Line Outage Identification using Decentralized State Estimation

**input** : $z_{j;t}$, $\epsilon$, $n$, case-data
**output** : $\hat{h}_t$ (Line under outage)
**Initialization** : $t \leftarrow 0, \hat{h}_t \leftarrow \hbar_0, \text{MAX}\mathcal{Z}^t_{\hat{h}_t} \leftarrow 0$,

$\quad \mathcal{Z}^t_{h_i h_j} \leftarrow O_{n+1 \times n+1}, \mathcal{Z}^{t-1}_{h_i h_j} \leftarrow O_{n+1 \times n+1}, e_{th}$

**while** $MAX\mathcal{Z}^t_{\hat{h}_t} < \log(\frac{n+1}{\epsilon})$ **do**

  **for** $i \leftarrow 0$ **to** $n$ **do**

    **Function** decentralizedSE($i,z_{j;t}$,case-data):
      **input** : Read $x_{j;t-1}, \Sigma_{j;t-1}$ from previous step
      **Initialize** : $Q_{j;t-1}, R_{j;t}, e_{j;t}$
      **while** $e_{j;t} < e_{th}, \forall j$ **do**
        **for** $j \leftarrow 1$ **to** $L$ **do**
          **Function** ukfSE($j, x_{j;t-1}, \Sigma_{j;t-1}$, $z_{j;t}$):
            Run the local state estimation using UKF to obtain $\hat{x}_{j;t}$ and $\hat{\Sigma}_{j;t}$ using Equations (19) to (30)
            **return** $\hat{x}_{j;t}, \hat{\Sigma}_{j;t}, e_{j;t}$
        **end**
        Construct $H(j,t)$ and $\mathfrak{I}(j,t)$ using $\hat{x}_{j;t}, \hat{\Sigma}_{j;t}$
        Perform max- and min-consensus procedure to obtain $\tilde{H}(j,t)$ and $\tilde{\mathfrak{I}}(j,t)$
        Given $\tilde{H}(j,t), \tilde{\mathfrak{I}}(j,t)$ obtain $\tilde{x}_{j;t}, \tilde{\Sigma}_{j;t}$
        **for** $j \leftarrow 1$ **to** $L$ **do**
          **Function** ukfSE($j, \tilde{x}_{j;t}, \tilde{\Sigma}_{j;t}, z_{j;t}$):
            Run the local state estimation using UKF to obtain $x_{j;t}$ and $\Sigma_{j;t}$ using Equations (19) to (30)
            $x_{j;t-1} \leftarrow x_{j;t}, \Sigma_{j;t-1} \leftarrow \Sigma_{j;t}$
            **return** $x_{j;t-1}, \Sigma_{j;t-1}, e_{j;t}$
        **end**
      **end**
    **End Function**
    $\Omega_t \leftarrow \text{diag}[\Omega_{1;t}, \ldots, \Omega_{L;t}]$
    $e_t \leftarrow [e_{1;t}, \ldots, e_{L;t}]$
  **end**
  **for** $i \leftarrow 0$ **to** $n$ **do**
    **for** $j \leftarrow 0$ **to** $n$ **do**
      Compute Elements of $\mathcal{Z}^t_{h_i h_j}$    // Eq. (45)
    **end**
  **end**
  $\mathcal{Z}^t_{h_i h_j} \leftarrow \mathcal{Z}^{t-1}_{h_i h_j} + \mathcal{Z}^t_{h_i h_j}$
  $\mathcal{Z}^t_h \leftarrow \min_{\hbar' \neq \hbar} \mathcal{Z}^t_{\hbar\hbar'}$
  $\text{MAX}\mathcal{Z}^t_{\hat{h}_t} \leftarrow \max_{\hbar}(\mathcal{Z}^t_h)$
  $\hat{h}_t \leftarrow \arg\max_h \mathcal{Z}^t_{\hbar}$
  $t \leftarrow t + 1$
**end**
**return** $\hat{h}_t$